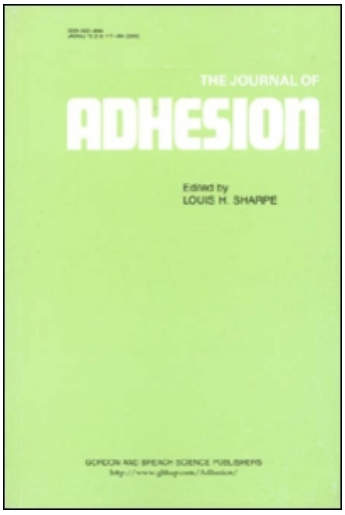

The Journal of Adhesion
Publication details, including instructions for authors and subscription information:
http://www.informaworld.com/smpp/title~content=t713453635

Theoretical Investigation of Acid-Base Properties of Oxide Surfaces

C. Noguera[a]
[a] Laboratoire de Physique des Solides, associé au CNRS, Université Paris Sud, Orsay, France

To cite this Article Noguera, C.(1996) 'Theoretical Investigation of Acid-Base Properties of Oxide Surfaces', The Journal of Adhesion, 57: 1, 91 — 114
To link to this Article: DOI: 10.1080/00218469608013646
URL: http://dx.doi.org/10.1080/00218469608013646

J. Adhesion, 1996, Vol. 57, pp. 91–114
Reprints available directly from the publisher
Photocopying permitted by license only

Theoretical Investigation of Acid-Base Properties of Oxide Surfaces*

C. NOGUERA

Laboratoire de Physique des Solides, associé au CNRS, Université Paris Sud, 91405 Orsay (France)

(Received November 21, 1994; in final form March 30, 1995)

We analyze the acid-base strength of oxide surfaces, in the light of quantum calculations of proton and hydroxyl group adsorption on oxides presenting a wide range of ionicities and surface orientations. The parameters which determine the values of the charge transfers, adsorption energies and structural properties of surface OH groups are discussed and related to the indicators generally used to quantify acid-base reaction strength in adhesion science, heterogeneous catalysis and colloid physics.

KEY WORDS: oxide surfaces; Brønsted acidity; Lewis acidity; surface hydroxylation; OH stretching frequencies; quantum calculations

1 INTRODUCTION

Due to its various aspects and the difficulty of the questions it raises, the science of adhesion brings together specialists from several disciplinary fields: mechanics of solids, polymer science, surface physics, chemistry, etc. One important point, among others, is the understanding of the nature and strength of the interfacial bonds formed between the adhesive and the substrate, which govern the joint strength and durability. The recognition that, in the contact zone, bonds are formed thanks to proton or electron exchange, has led the scientists to use the concepts of Brønsted and Lewis acidity, originally developed for interactions between molecules in a solvent. Because solid surfaces present more degrees of freedom than small molecules, it was necessary to reconsider the traditional concepts used in this field, and there has thus been a renewal of studies of acid-base processes in the context of adhesion science.[1,2] Similar developments have been made in other fields of research, such as heterogeneous catalysis, colloid physics, etc.

In petrochemistry and organic synthesis, for example, solid acids have been used for a long time. More recently, several types of solid bases have been discovered and used as catalysts.[3,4] Oxides occupy a prominent position among solid catalysts, and have, thus, been the object of many studies over the last thirty years.

In colloid physics, ion exchanges take place at the interface between the particles and the liquid in which they are in suspension, leading to surface charging. The counter-ions

* One of a Collection of papers honoring Jacques Schultz, the recipient in February 1995 of *The Adhesion Society Award for Excellence in Adhesion Science, Sponsored by 3M.*

in the solution screen this charge and "dress" the particles. The interfacial reactions are, thus, responsible for the strength and nature of the long range interactions between particles, *i.e.* they govern the stability of the colloidal suspension.[5] Since exchanges of protons or hydroxyl groups at the interfaces often take place, acid-base theories have also been developed in this field.

One of the basic questions underlying all studies is: "which are the specific properties of the reactants that determine the strength of an acid-base reaction". As far as oxides are concerned, depending upon the field of research, various physical parameters have been proposed: the cation electronegativity, the cation ionic radius and formal charge, the oxygen partial charge, the surface site coordination; various experimental indicators are also used: the adsorption energy of test molecules in catalysis, the isoelectric point of the surface—also called point of zero charge—in electrochemistry, the stretching frequencies of surface OH groups, etc. Nevertheless, the link between these parameters and the surface acidity relies, in most cases, upon either very qualitative or empirical models.

Due to the development of advanced numerical methods in the last decades, quantum approaches are now able to describe accurately the chemical bonds formed between two reactants. Nevertheless, when a surface is involved, the actual systems met in the applications cannot yet be simulated, for example, a dense polymeric layer adsorbed on a rough surface, because this would require too large memory sizes or too long computation times. Quantum calculations, thus, cannot compete with empirical models in the prediction of adhesion strengths. Yet, they may allow one to check their validity in model cases, for example, small molecules adsorbed on a substrate, or large molecules adsorbed on a cluster of a few atoms which simulates the substrate. This has been done in a number of cases but, to our knowledge, mostly for adsorption processes on metallic surfaces.[6,7] Numerical results for the adsorption of molecules on oxide surfaces may be found in the literature,[8] but they have not been discussed in the framework of acid-base interactions.

It is the goal of this paper to discuss the parameters which determine the acid-base strength of oxide surfaces, in the light of simulations of elementary acid-base reactions. We have previously performed quantum calculations of the adsorption of protons and hydroxyl groups, with the aim of studying the dissociative adsorption of water on clean oxide surfaces.[9-11] We wish here to analyze these results in the framework of acid-base interactions, and discuss the applicability of empirical approaches to these adsorption processes. We will consider situations of increasing complexity: 1) a series of oxides presenting different ionicities, 2) several surface orientations of a given oxide, 3) two coverages of a given oxide surface. The paper is organized as follows: Section 2 reviews the qualitative or empirical models used when oxide surfaces are concerned; in Section 3, we summarize the results of our calculations of proton and hydroxyl group adsorption. A critical discussion is presented in Section 4.

2 RELEVANT PARAMETERS

In this section, we review the parameters used in the literature to account for the acid-base strength of an oxide: the cation formal charge and ionic radius, the surface

site coordination number, the cation electronegativity and the oxygen partial charge, the stretching frequency of surface OH groups and the oxygen core level shift.

2.1 Cation Formal Charge and Ionic Radius

The Brønsted acidity of an hydroxylated surface is defined as the ability of the surface to capture or donate protons, according to the reactions:

$$MOH \rightarrow MO^- + H^+, \tag{2.1}$$

and:

$$MOH + H^+ \rightarrow MOH_2^+ \tag{2.2}$$

With the equilibrium constants, K_1 and K_2, of these two reactions are associated an acid pK_1 and a basic pK_2. Using electrochemical measurements, it is possible to determine the pH of the solution in contact with the surface which yields an equal number of positively and negatively charged surface sites: $[MOH_2^+] = [MO^-]$. This pH value is called the isoelectric point of the surface (*IEPS*); it is determined by a proton concentration equal to:

$$[H^+]^2 = \frac{K_1}{K_2} \tag{2.3}$$

The *IEPS* is related to the variation of the standard free energy, ΔG^0, of the global reaction $MO^- + 2H^+ \rightarrow MOH_2^+$:

$$IEPS = \frac{1}{2}\left(\frac{-\Delta G^0}{2.3RT}\right) \tag{2.4}$$

A high *IEPS* reveals a strong surface basicity, while an *IEPS* close to zero is characteristic of a strong acidity. Parks[12] has compiled the *IEPS* of many oxides. He has shown their relationship with the ratio Q_M/r_M between the cation formal charge and its ionic radius. He was able to classify oxides according to decreasing *IEPS*, as a function of Q_M, as shown in Table I.

The basic oxides involve cations with the lowest formal charge: they are alkaline or alkaline-earth oxides. At the opposite extreme, the cation formal charges of acidic oxides are high (+5 or +6). *IEPS* values display a saturation value close to zero, because water, which is the solvent in which *IEPS* measurements are made, does not

TABLE I
Typical range of values of oxide *IEPS*

M_2O	$Q_M = +1$	$11.5 < IEPS$
MO	$Q_M = +2$	$8.5 < IEPS < 12.5$
M_2O_3	$Q_M = +3$	$6.5 < IEPS < 10.4$
MO_2	$Q_M = +4$	$0.5 < IEPS < 7.5$
M_2O_5	$Q_M = +5$	$IEPS < 0.5$
MO_3	$Q_M = +6$	$IEPS < 0.5$

allow one to study species more acidic than H_3O^+. Parks has established that *IEPS* is roughly a linear decreasing function of the ratio Q_M/r_M. Following a similar idea, in the context of heterogeneous catalysis, Auroux and Gervasini[13] have shown that the mean CO_2 adsorption energy on oxides increases, which reveals an increased basic character, when the ratio Q_M/r_M diminishes.

A simple electrostatic model, due to Parks, accounts for the relationship between the *IEPS* and the ratio Q_M/r_M. Parks assumed that the free energy variation, ΔG^0, which determines the *IEPS* (Eq. (2.4)), is mainly due to the work of the electrostatic forces involved when protons approach or leave the surface. Assuming, in addition, that ions bear integer point charges, and that the interaction between the oxygen and the closest surface cation prevails, he deduced that:

$$\Delta G^0 = \frac{2Q_O Q_H}{\varepsilon r_O} + \frac{2Q_M Q_H}{\varepsilon(2r_O + r_M)} + \Delta G' \tag{2.5}$$

an expression in which $Q_O = -2$ and $Q_H = +1$, ε is the oxide dielectric constant, and r_O and r_M are the oxygen and cation ionic radii, respectively. The first term in Equation (2.5) represents the attractive interaction between the proton and the surface oxygen and the second term its repulsive interaction with the neighboring cation. Parks assumed that the free energy of non-electrostatic origin, $\Delta G'$, remains a constant whatever the oxide. Since only the proton-cation interaction distinguishes the different oxides in this model, *IEPS* may be written under the most general form:

$$IEPS = A - B\frac{Q_M}{(2r_O + r_M)} \tag{2.6}$$

This equation accounts for the higher acidity of oxides involving cations with a high formal charge and a small ionic radius. The *IEPS* values have been used in a model of adhesion of polar polymers on oxide surfaces.[14]

2.2 Surface Site Coordination Number

The electrostatic model, presented above, predicts the same acid strength for all surface sites of a given oxide. Yet, the *IEPS* value may strongly depend upon the orientation of the face in contact with the electrolyte. For example, Nabavi *et al.*[15] have shown that the (100), (110) and (111) faces of nanometric-size particles of cerium oxide, CeO_2, have very different pK_1 and pK_2. They related this result to the different nature of the surface sites: on the hydroxylated (100) face, oxygens with coordination number $Z = 2$ are found, which belong either to the ideal surface or to adsorbed OH^- groups (we keep the denomination "oxygen sites" for oxygen atoms belonging to the oxide surface, as in most surface science papers, rather than "oxide sites" which is used by some authors when they wish to discriminate O^{2-} from $O_2(g)$ species; the presence of adsorbed oxygen molecules will never be considered in this paper). On the two other faces, the oxygens are three-fold coordinated on the ideal surface or singly coordinated in the case of an *on-top* adsorption of an OH^-.

Parks' electrostatic model was extended to account for the surface site environment. We give below the arguments underlying the so-called MUSIC model (MU-

SIC = multisite complexation model).[16,17] As in Parks' model, electrostatic forces are assumed to be reponsible for the proton adsorption or desorption, but, in order to take into account in an effective way the potentials exerted by the ligands surrounding the oxygen atom, bond charges equal to $q = Q_M/Z_b$ (Z_b is the cation coordination number in the bulk) are introduced.[18-19] The free energy associated with each elementary protonation reaction on a surface then takes a form very similar to that proposed by Parks:

$$\Delta G^0 = 2\frac{Q_O Q_H}{\varepsilon R_{OH}} + \frac{2Q_H Z_q}{\varepsilon R_{HM}} + \Delta G' \tag{2.7}$$

Z is the oxygen coordination number and R_{OH} and R_{HM} are the proton-oxygen and proton-cation interatomic distances. R_{HM} is assumed to be equal to the anion-cation interatomic distance in the oxide. The main difference between Equation (2.7) and Parks' formula (Eq. (2.5)) lies in the value of the effective positive charge: here, each of the Z cation neighbors gives a contribution equal to q. The pK associated with acid or basic reactions, thus, depends in a linear way upon the oxygen coordination number, Z:

$$pK = A - B\frac{Z_q}{R_{HM}} \tag{2.8}$$

The A and B constants are fitted to reproduce the behavior of the corresponding molecules in solution. The MUSIC model predicts that the basicity of the surface oxygens increases as their coordination number decreases, while the acidity of OH groups increases as their coordination number increases.

2.3 Cation Electronegativity and Oxygen Partial Charge

Another parameter which is often referred to, when quantifying the acidity of an oxide, is the cation electronegativity. It is defined as minus the first derivative of the atom energy, E, with respect to its electron number, N: $\chi_M = -\partial E/\partial N$. Its relevance is easily conceived since, according to Lewis' definition, the acidity is the ability to receive an electron pair: the acidity is, thus, expected to be higher for cations of higher electronegativity. In a given oxide series, the higher the cation in the periodic table, the stronger the oxide acidity; the more on the left of the periodic table the cation is located, the more basic the oxide.

It was recognized that it is not the *neutral* atom electronegativity which has to be considered, but rather the electronegativity of the atom with its actual charge state in the oxide. Following ideas developed by Iczkowski and Margrave,[20] Tanaka and Ozaki[21] have shown that, as a first approximation, *i.e.* when assuming that the ion energy, E, is a quadratic function of N, the electronegativity χ_M reads:

$$\chi_M = \chi_{M0}(1 + 2aQ_M) \tag{2.9}$$

χ_{M0} is the electronegativity of the neutral atoms. χ_M varies linearly with the cation charge, Q_M; the coefficient $a = (3I_1 - I_2)/(I_2 - I_1)$ is related to the values of the first and

second ionization potentials, I_1 and I_2. It is close to 1 in a large part of the periodic table.

Tanaka and Ozaki have proved that the pK_a of the ionization reaction of a solvated cation:

$$M(H_2O)_m^{\alpha+} + H_2O \rightarrow [M(H_2O)_{m-1}OH]^{(\alpha-1)+} + H_3O^+ \qquad (2.10)$$

varies monotonically with χ_M, and that the same is true for the oxide *IEPS* and for the catalytic activity in the reactions of propylene hydration, iso-butylene polymerization and acetaldehyde polymerization. Similarly, Connell and Dumesic have found that adding iron on a silica surface generates acidic sites, the strongest of which are due to Fe^{3+} ions and the weakest ones to Fe^{2+} species.[22,23] They relate this behavior to the higher electronegativity of Fe^{3+} ions. It is not surprising to find a good correlation between the oxide *IEPS* and the cation electronegativity since, when comparing different oxides, the charge value Q_M induces the largest changes in χ_M. Yet, one should remember that the microscopic processes underlying Parks' model and the electronegativity argument are different: the first one only considers the electrostatic interactions, while the second is related to the ability of a cation to form a strong covalent bond.

In oxides, the ionicity of the anion-cation bond is strongly correlated to the cation electronegativity: as χ_M increases, the covalent character of the cation-oxygen bond increases and the absolute value of the oxygen effective charge, Q_O, decreases: Sanderson[24] has proposed an empirical method to estimate the partial charges in mixed iono-covalent bonds, which assumes that the anion-cation charge transfer equalizes the electronegativities, χ, of the two species. For example, he finds that $|Q_O|$ decreases in the series: Na_2O, MgO, Al_2O_3, SiO_2 and SnO_2. In the literature, a correlation between the oxide acidity and the oxygen partial charge has been established. For example, Tanabe and Fukuda,[25] by measuring the CO_2 adsorption energy in the series of alkaline-earth oxides, have found that the basicity decreases from BaO to MgO; in the same series, according to Sanderson, the oxygen partial charges are, respectively, equal to -0.61, -0.60, -0.57 and -0.50. The correlation was confirmed by Auroux and Gervasini[13] who showed that the adsorption energy of NH_3, on a large number of oxides, decreases when the percentage of ionic character—defined according to Sanderson's scale[26] –increases, while the adsorption energy of CO_2 increases along the same series.

Sanderson[24] also introduced the atom environment in his estimation of the effective charges. In the fluoride series, he showed that the fluorine partial charge, Q_F, decreases in absolute value when the anion coordination number, Z, decreases: for example, $Q_F = -0.89$ in CsF ($Z = 6$), $Q_F = -0.56$ in BaF_2($Z = 4$), $Q_F = -0.29$ in BeF_2($Z = 2$) and $Q_F = -0.17$ in SiF_4($Z = 1$). A similar result can be derived for oxides.

2.4 Stretching Frequencies of Surface OH Groups

Infra-red absorption and HREELS experiments give access to the stretching frequencies, ν_{OH}, of OH species on surfaces. When water, bases, or acids are dissociated on a surface, several types of OH^- groups are formed: some result from the adsorption of protons on surface oxygens; others are free OH groups adsorbed on surface cations.[27] Two parameters induce changes in the OH structural properties: the surface site

coordination number, Z, and the number of bonds, Z_a, between the OH group and the surface. There exist some qualitative correlations between the stretching frequency shift, the nature of the adsorption site, and the surface acidity:[28-29]

- Stretching frequencies of hydroxyl groups bound to surface cations are higher than those of interfacial OH groups due to the adsorption of protons on surface oxygens. On rough surfaces, these two families present many internal splittings, due to all possible values of Z and Z_a, and due to the effects of lateral interactions between adsorbed groups.
- The stretching frequency of an hydroxyl group adsorbed on a single surface cation is lower when the cation coordination number, Z, is lower. The reverse is true for a proton adsorbed on a surface oxygen.
- On a given compound, the lower the stretching frequency, the weaker the O—H bond, and the less basic the oxygen. For hydroxyl groups adsorbed on a surface cation, the lower ν_{OH} the stronger the OH-cation bond and the more acidic the cation. This rule is not always obeyed when two different compounds are compared.

2.5 Oxygen Core Level Shift

It has been noticed that the position of the oxygen 1*s* core level is shifted towards higher and higher binding energies as the oxide basicity decreases. For example, Vinek *et al.*[30] used this criterion to classify the following oxides from the more basic to the more acidic: La_2O_3(529 eV) > Sm_2O_3(529.2 eV) > CeO_2(529.4 eV) = Dy_2O_3(529.4 eV) > Y_2O_3(529.5 eV) > Fe_2O_3(530.3 eV) > Al_2O_3(531.8 eV) > GeO_2(532.4 eV); P_2O_5 (532.4 eV) > SiO_2(533.1 eV). Values in brackets give the measured oxygen 1*s* binding energies. They explained their results within the framework of Sanderson's partial charge model, and showed that an increase in the basicity is associated with a larger oxygen partial charge.

A correlation has also been established between the oxygen 1*s* core level shift and the *IEPS* in various oxides.[31-33]

Although not exhaustive, this overview presents the parameters which are most often used in the literature to analyze acid-base experiments on oxide surfaces. We will consider them again in the last section to discuss the numerical results of the adsorption of protons and hydroxyl groups, which are now presented.

3 ADSORPTION OF PROTONS AND HYDROXYL GROUPS ON OXIDE SURFACES

When studying the dissociative adsorption of water on oxide surfaces, we have considered several series of surfaces: a first series: BaO(100), SrO(100), CaO(100), MgO(100), TiO_2(110) (rutile), and SiO_2(0001) (α-quartz)[9] along which the oxide ionicity decreases, and three MgO surface orientations: (100), (110) and (211),[10] with different surface site coordination numbers, Z—the surface atoms are respectively five-, four- and three-fold coordinated. Although only the (100) face is stable in most rock salt oxides, adsorption on the two other surfaces may give hints of what happens

on defect sites in real materials. We have also considered all these systems in the limit of saturation of the surface by dissociated water molecules.[11]

The protons adsorb on-top of an oxygen on all surfaces, because the small size of the proton prevents the formation of two bonds with surface atoms. In the first series of oxides, the hydroxyl groups adsorb on a single surface cation ($Z_a = 1$) with its oxygen at the position of a missing lattice oxygen. In the second series, they may bind to several cations: on MgO(100) the most likely adsorption configuration is on-top ($Z_a = 1$) while, on the (110) face, the OH^- groups may adsorb on-top ($Z_a = 1$) or on-bridge ($Z_a = 2$), and on the (211) face they may adsorb on-top ($Z_a = 1$), on-bridge ($Z_a = 2$) or in a ternary site ($Z_a = 3$). Yet, the adsorption sites characterized by the largest value of Z_a are always the most stable and we will only discuss them in the following.

The numerical method relies on a semi-empirical, self-consistent, tight-binding approach, at the Hartree-Fock level, which treats the electrostatic and covalent processes on the same level. The details of the method have been published elsewhere.[9,11] In some specific cases, the electronic structure calculation is coupled to a geometry optimization code, which computes the forces acting on the atoms using the Hellmann-Feynmann's theorem and uses the conjugate gradient method to search for the atomic configuration with the lowest energy.

The adsorptions of protons and hydroxyl groups represent elementary acid-base reactions involving a surface. The calculations yield several quantities which are relevant in the context of acid-base interactions: the charge transfers along the interfacial bonds, the adsorption energies and the geometric characteristics of the OH groups when the optimization procedure is used. The first quantity is directly related to the Lewis acidity or basicity, *i.e.* to the ability to give or receive electrons; the second is of interest to discuss, *e.g.*, the *IEPS* value, which is related to the free energies of protonation reactions, or the Brønsted acidity. By considering various oxides, various surface orientations and two adsorbate densities, it is possible to discuss the acid-base strength as a function of the oxide ionicity, as a function of the nature of the surface sites and as a function of the surface coverage.

3.1 Charge Transfers

We first comment on the values of the charge transfers which take place between the adsorbed species and the surfaces. They have been calculated under the assumption of a rigid geometry: the O—H interatomic distance, d_{OH}, equal to 0.957 Å and the oxygen of the hydroxyl group at the position of a missing lattice oxygen.

Table II gives the value of the electron transfers, n_{H+}, from the surface to the proton and Δn_{OH} from the hydroxyl group to the surface, in the series of oxides, in the limit of zero coverage. It shows that n_{H+} decreases as the oxide ionicity decreases, while Δn_{OH} increases and reaches especially high values for TiO_2 and SiO_2.

Table III gives the charge transfers on the three MgO surfaces: while n_{H+} remains roughly constant in the series, Δn_{OH} increases. Yet, it may be noticed that, since the number of bonds, Z_a, between the adsorbate and the surface increases linearly in the series ($Z_a = 1, 2$ and 3, respectively), the charge transfer *per bond*, $\Delta n_{OH}/Z_a$, is nearly independent of the surface orientation.

TABLE II
Proton and hydroxyl group adsorption on rigid oxide surfaces in the limit of zero coverage: n_{H+} and Δn_{OH} are, respectively, the electron transfers from the surface to the proton and from the hydroxyl group to the surface

	BaO(100)	SrO(100)	CaO(100)	MgO(100)	TiO_2(110)	SiO_2(0001)
n_{H+}	0.83	0.81	0.78	0.76	0.65	0.60
Δn_{OH}	0.07	0.08	0.11	0.13	0.54	0.88

TABLE III
Proton and hydroxyl group adsorption on the three rigid MgO(100), (110) and (211) faces, in the limit of zero coverage. Same notations as in Table II

MgO	(100)	(110)	(211)
n_{H+}	0.76	0.76	0.77
Δn_{OH}	0.13	0.26	0.34

In the limit of full saturation of the surfaces by dissociated water molecules, there is a modification of the charge transfers: in the series of oxides (Table IV), the interaction between adsorbates induces an important weakening of the surface-proton charge transfer, n_{H+}, on rock salt surfaces (about 0.15 electron), but nearly no variation on TiO_2 and SiO_2. An effect of opposite sign is found for Δn_{OH}, which becomes much larger on rock salt surfaces and decreases slightly on rutile and quartz. Yet, the qualitative variations of n_{H+} and Δn_{OH} along the series remain unchanged, whatever the density of adsorbates.

For the three MgO surfaces (Table V), the interaction between adsorbates yields modifications of the charge transfers: n_{H+} decreases and Δn_{OH} increases. The modifications are strong at the beginning of the series, on MgO(100) where the density of the hydroxylation layer is the highest.

As far as electron transfers are concerned, it may thus be concluded that the Lewis acidity of the oxides from BaO to SiO_2 increases, both because their surface oxygens

TABLE IV
Proton and hydroxyl group adsorption on rigid oxide surfaces, in the limit of saturation by dissociated water molecules. Same notations as in Table II

	BaO(100)	SrO(100)	CaO(100)	MgO(100)	TiO_2(110)	SiO_2(0001)
n_{H+}	0.67	0.65	0.61	0.59	0.63	0.63
Δn_{OH}	0.31	0.33	0.36	0.40	0.47	0.75

TABLE V
Proton and hydroxyl group adsorption on rigid MgO (100), (110) and (211) surfaces, in the limit of saturation. Same notations as in Table II

MgO	(100)	(110)	(211)
n_{H+}	0.59	0.66	0.74
Δn_{OH}	0.40	0.33	0.33

donate less and less electrons to the protons and because their surface cations accept more and more electrons from the hydroxyl groups. This trend may be correlated with the increasing covalent character of the cation-oxygen bond in the series. The conclusion does not depend upon the adsorbate density, which only changes the strength of the adsorbate-substrate acid-base interaction: the basicity of rock salt oxides and the acidity of rutile and quartz decrease when the coverage of the surface increases.

On the three MgO faces, the charge transfer *per bond* does not depend much upon the surface orientation in the limit of zero coverage. When the density of adsorbates becomes large, the conclusion is modified, and it is found that surfaces become more and more basic as the coordination number of the surface atoms decreases.

3.2 Adsorption Energies

The values of the adsorption energies, E^{ads}_{H+} and E^{ads}_{OH-}, of protons and hydroxyl groups in the series of oxides and on the three MgO faces are now presented. They are given in Table VI and in Table VII, respectively.

TABLE VI
Proton and hydroxyl group adsorption energies (in eV) on oxide surfaces in the limit of zero coverage (top part) and at full saturation (lower part). E^{ads}_{tot} is the sum of $E^{ads}_{H^+}$ and $E^{ads}_{OH^-}$. E^{ads} is the adsorption energy per dissociated water molecule on fully hydroxylated surfaces

	BaO(100)	SrO(100)	CaO(100)	MgO(100)	TiO_2(110)	SiO_2(0001)
$E^{ads}_{H^+}$	10.7	10.1	9.3	8.3	5.9	4.8
$E^{ads}_{OH^-}$	0.4	0.0	0.3	1	8.3	10.3
E^{ads}_{tot}	11.1	10.1	9.6	9.3	14.2	15.1
E^{ads}	12.7	12.2	12.1	12.3	16.6	21.0

TABLE VII
Proton and hydroxyl group adsorption energies (in eV) on MgO (100), (110) and (211). Same notations as in Table VI

MgO	(100)	(110)	(211)
E^{ads}_{H+}	8.3	9.1	11.6
E^{ads}_{OH-}	1.0	2.4	4.9
E^{ads}_{tot}	9.3	11.5	16.5
E^{ads}	12.3	15.8	19.7

The top parts of the tables refer to the limit of zero coverage. E_{tot}^{ads} is the sum of E_{H+}^{ads} and $E_{OH^-}^{ads}$. The strength of the interactions between adsorbates may be deduced from a comparison of E_{tot}^{ads} (limit of zero coverage) and E^{ads} (full saturation), this latter being given in the lower part of the tables.

Along the series of oxides, the proton adsorption energy decreases while the hydroxyl group adsorption energy increases. This trend is consistent with the changes in the charge transfers discussed above. A non-monotonic variation of E_{tot}^{ads} results: E_{tot}^{ads} decreases along the rock salt series but becomes large again for rutile and quartz. In the limit of saturation, E^{ads} is roughly constant in the rock salt series and is large for rutile and quartz.

For the three MgO surfaces, both the proton and the hydroxyl group adsorption energies increase, and so do E_{tot}^{ads} and E^{ads}. One can note that, in both the oxide series and the MgO series, the interactions between adsorbates generally stabilize the adsorption configurations.

To summarize, as far as adsorption energies are concerned, it is found that an increased covalent character of the oxides is associated with a larger acidity: the surface oxygens are less basic and the surface cations more acidic. The adsorption energies on the three MgO faces, on the other hand, do not follow the same trends as the charge transfers: on the basis of the adsorption energy criterion, the oxygens are more basic and the magnesiums more acidic in the series. This result agrees with the MUSIC model and with the statement that more under-coordinated sites are generally more reactive.

3.3 Surface OH Structural Characteristics

We have used the geometry optimization procedure to calculate the structural characteristics of adsorbed protons and hydroxyl groups on the three MgO faces. The values of the O—H interatomic distances are given in Table VIII in which d_{OH+} denotes the interfacial O-proton bond length and d_{OH} the O—H interatomic distance inside the hydroxyl group. The top part of the table refers to the limit of zero coverage, while the lower part describes the fully-saturated surfaces. We have also given the corresponding values of the proton and of the OH terminal hydrogen electron numbers, n_{H+} and n_H, respectively, in the right part of the table. One should note that, as expected, the values of n_{H+} obtained after the geometry optimization, which are given in Table VIII, are different from those characteristic of a rigid geometry, which were written in Tables III

TABLE VIII

O—H bond lengths, in Ångstroms, along the interfacial oxygen-proton bonds (d_{OH^+}) and inside the adsorbed hydroxyl groups (d_{OH}). The top part deals with the limit of zero coverage, while the lower part is relevant for full saturation. The right part of the table gives the associated values of the hydrogen electron numbers

MgO	(100)	(110)	(211)	MgO	(100)	(110)	(211)
d_{OH^+}	0.963	0.961	0.958	n_{H^+}	0.77	0.77	0.76
d_{OH}	0.960	0.960	0.964	n_H	0.85	0.80	0.76
d_{OH^+}	0.991	0.972	0.964	n_{H^+}	0.62	0.70	0.74
d_{OH}	0.982	0.966	0.964	n_H	0.66	0.73	0.75

and V; nevertheless, the difference is small and does not alter the trends for the charge transfers discussed above.

In the limit of zero coverage, the O—H and OH^+ bond lengths are very close to the interatomic distance in the free hydoxyl group ($d_{OH} = 0.957$ Å). They vary little with the surface orientation. The result is different at full coverage where both d_{OH+} and d_{OH} decrease significantly in the series. A clear correlation between the O—H bond lengths and the hydrogen electron numbers appears in Table VIII: a bond length expansion takes place whenever the oxygen-hydrogen electron transfer decreases.

4 DISCUSSION

In order to rationalize the numerical results presented above, we now present analytical arguments which specify the concept of ionicity in mixed iono-covalent materials, which allow one to extract the relevant parameters governing the adsorbate-substrate charge transfers and adsorption energies and which explain the link between the surface acidity and the geometric properties of adsorbed hydroxyl groups.

4.1 Ionicity of the Oxygen-cation Bond in an Oxide

We wish first to address three points, related to the electronic structure of oxides *in the absence* of adsorbates, which are closely related to the arguments of electronegativity and partial charge developed in Section 2. First, we will show that, in an oxide, the concept of electronegativity has to be enlarged to account for the long-range electrostatic interactions between ions. Second, we will develop a model for the oxygen partial charge, relying upon the resolution of a simplified quantum Hamiltonian, rather than on empirical arguments. Third, we will comment on the variations of the surface charges as a function of the surface orientation.

In oxides, the oxygens and cations bear charges of opposite signs, which induce strong electrostatic potentials on the electrons. A correction to the atomic orbital energies $\varepsilon_i^0 (i = M, O)$ of the neutral atoms results, which depends upon the ionic charges, Q_i, and upon the atomic structure. Under the most simplifying Hartree approximation, when the eigenstates of the Hamiltonian are developed on an atomic orbital basis set, the diagonal terms of the Hamiltonian matrix, which represent effective atomic orbital energies, read (in atomic units):

$$\varepsilon_i = \varepsilon_i^0 - U_i Q_i - V_i \tag{4.1}$$

with $-U_i Q_i$ the intra-atomic correction associated with the excess (on the oxygens) or loss (on the cations) of electron-electron repulsion (U_i is the intra-atomic electron-electron repulsion integral), and V_i the electrostatic potential, called the Madelung potential, exerted on atom i by all other ions. This expression may be used to estimate the ion internal energy, E_i, and to write down the Mulliken electronegativity, $\chi_i = -\partial E_i / \partial N_i$; assuming that a single outer atomic orbital is involved in the chemical bond, χ_i reads:

$$\chi_i = \chi_{i0} + U_i Q_i + V_i \tag{4.2}$$

This expression of χ_i contains a correction due to intra-atomic electron-electron interactions, as in References 20 and 21, although, in Equation (4.2), the effective charge rather than the formal charge has to be used. In addition, solid state effects give a contribution to χ_i, equal to the Madelung potential, V_i. Equation (4.2), thus, gives a generalization of the concept of electronegativity, suited to processes which take place in a solid or on a surface. It accounts for the variations of electronegativity as a function of the charge state and as a function of the site environment. In this latter case, the variations of χ_i are driven by the changes in the Madelung potential. For example, in absolute value, V_i is smaller on surface atoms than on bulk atoms. It also decreases as the Miller indexes of the surfaces become larger, because the density of atoms in the surface plane becomes lower. As a result, the cation electronegativity is higher on more open surfaces while the oxygen electronegativity is lower.

Equations (4.1) and (4.2) show that, in a Hartree scheme, there is a direct correspondence between χ_i and the position of the effective outer levels, ε_i. The effective atomic energies, ε_i, strongly determine the electron sharing between cations and oxygens in oxides. We have recently developed a quantum model[34, 35] suited to binary oxides of stoichiometry M_nO_m, in which the atoms occupy the sites of an alternating lattice,[37, 38] which gives an explicit expression of the partial charges. This model is recalled in the Appendix. It is a tight-binding analytical approach, which relies on several assumptions: i) all the oxygens are assumed to have the same outer level effective energy, ε_O, and a similar hypothesis is made for the cations; ii) the non-diagonal terms of the Hamiltonian, β, called resonance integrals, which represent the probability of hopping of electrons between two atoms, are considered only when neighboring atoms of opposite types are involved; iii) finally, only local orbital hybridization is taken into account and long range band effects are neglected.[34] This model yields a simplified expression for the oxygen-cation charge transfer:

$$\delta Q = \frac{n_0}{m}\left(1 - \frac{\varepsilon_M - \varepsilon_O}{\sqrt{(\varepsilon_M - \varepsilon_O)^2 + 4Z\beta^2}}\right) \tag{4.3}$$

with n_0 the number of oxygen orbitals coupled to the cation levels and Z the oxygen coordination number. According to Equation (4.3), the absolute value of the oxygen charge, $|Q_O| = 2 - \delta Q$, is a decreasing function of the ratio $Z\beta^2/(\varepsilon_M - \varepsilon_O)^2$: when no electron delocalization occurs ($\beta = 0$), the oxide is fully ionic; the covalency of the oxygen-cation bond increases as β gets larger or as the energy difference $\varepsilon_M - \varepsilon_O$ decreases. This model was checked for all the oxides considered here, by carefully comparing its predictions with the results of self-consistent numerical calculations.[34]

We have found that the absolute values of the oxygen charges are equal to 1.45, 1.43, 1.33, 1.24, 0.74 and 0.67 in the series: BaO(100), SrO(100), CaO(100), MgO(100), TiO_2(110) and SiO_2(0001). The reduction of $|Q_O|$ demonstrates that the cation-oxygen bond is more and more covalent: it is mainly due to the increase in the cation electronegativity, χ_M^0. Yet, two other effects are also relevant, although to a lesser extent. First, the cation ionic radius decreases in the series: this is directly reflected in the values of the oxygen-cation first-neighbor distance, R, and thus in the strength of the resonance integrals, β, and of the Madelung potentials. Second, ε_O also varies in the series because it is a self-consistent function of the charge Q_O. At this point it is

interesting to note that, in a given atom, parallel shifts of the outer and inner atomic levels generally occur. The correlation between the variations of the 1*s* core level shifts and the oxide ionicity pointed out by Vinek *et al.*[30] may be rationalized in that way, provided that one neglects the final state effects in the photoemission process.

While in the bulk the oxygen charge varies monotonically with the coordination number, Z (Equation 4.3), the same is not true at the surface: for a given material, on non-polar surfaces, it is generally found[38] that the surface charges are very close to the bulk ones, despite possibly large reduction of Z along some surface orientations. For example, we have found that $|Q_O|$ is equal to 1.24, 1.23 and 1.20 on MgO(100), (110) and (211), respectively. A similar result applies on step edges and kinks on MgO surfaces.[39] This effect comes from a reduction of the energy difference $\varepsilon_M - \varepsilon_O$, which roughly balances the decrease in Z in the expression of the charge. The reduction of the Madelung potentials on surfaces, noted above, is responsible for the level shifts: for example, the ratio of surface-to-bulk Madelung potentials is equal to 0.96, 0.88 and 0.65, respectively, on the (100), (110) and (211) faces of rock salt oxides.[40, 41] A shift of ε_M towards lower energies and ε_O towards higher energies results.

To summarize, the analytical quantum formulation of the ionicity of the oxygen-cation bond in oxides that we have proposed allows one to estimate the effective level positions and effective charges both in the bulk and at the surfaces. This represents an advance, compared with the empirical arguments found in the literature.

4.2 Adsorbate-substrate Charge Transfers

The analytical model quoted above gives the relationship between the oxygen-cation charge transfer and the ratio $Z\beta^2/(\varepsilon_M - \varepsilon_O)^2$ in the bulk and at the surface of an oxide. Although it cannot be directly applied to adsorption processes, a detailed analysis of the numerical results given in Section 3 shows that a parameter of the type $Z_a\beta^2/(\varepsilon_1 - \varepsilon_2)^2$ remains relevant, provided that one takes Z_a as the number of adsorbate-substrate bonds, β as the effective resonance integral between both species, and $\varepsilon_1 - \varepsilon_2$ as the energy difference between the donor and acceptor energy levels. We will successively discuss the parameters involved in these quantities.

Adsorbate-substrate bond length The adsorbate-substrate bond length controls the value of the resonance integrals, β: in the case of proton adsorption, there is no significant change of d_{OH+} in the various oxides, because the proton-surface bond length remains very close to the O—H interatomic distance in the hydroxyl group or in the water molecule. On the other hand, in the case of hydroxyl group adsorption, the oxygen atom belonging to the OH^- group comes at a position close to that of a missing lattice oxygen: the O-cation distance is, thus, roughly a linear function of the cation ionic radius.

The adsorbate-substrate bond length also controls the value of the Madelung potential, V_i, exerted by one species on the other, which renormalizes the effective atomic levels ε_1 and ε_2, as indicated in Equation (4.1).

Number of adsorbate-substrate bonds As already mentioned, a proton cannot form multiple bonds with a planar oxide surface, because its radius is too small to allow a

close approach to two surface oxygens: on all surfaces, $Z_a = 1$. On the other hand, the oxygen of a hydroxyl group may bind to several cations: the Z_a value, thus, depends upon the surface orientation and upon the presence of surface irregularities.

Energy difference between the acceptor and donor levels The presence of the energy difference, $\varepsilon_1 - \varepsilon_2$, between the acceptor and donor levels in the denominator of $Z_a\beta^2/(\varepsilon_1 - \varepsilon_2)^2$, says that the charge transfer, δQ, increases when $\varepsilon_1 - \varepsilon_2$ gets smaller. For proton adsorption, ε_1 is the hydrogen 1*s* atomic energy, and ε_2 the surface oxygen 2*p* atomic energy. For OH^- adsorption, ε_1 is the energy of the surface cation outer level and ε_2 the energy of the OH^- oxygen 2*p* level. These level energies have to be estimated with the proper values of the partial charges on the atoms and of the Madelung potential corrections: in a Hartree scheme, the energy difference $\varepsilon_1 - \varepsilon_2$, thus, depends upon the cation electronegativity, the surface oxygen charge, the oxide structure, the surface orientation and the surface coverage:

- as the cation electronegativity increases in the first oxide series, ε_1 shifts to lower energies and gets closer to the energy ε_2 of the OH group; the charge transfers, Δn_{OH}, increase.
- along the same series, the surface oxygen level, ε_2, shifts towards lower energies as a result of the reduction of $|Q_O|$. A weakening of the oxygen-proton electron transfer results.
- the Madelung corrections to the atomic level position have to be carefully considered when several surfaces of a given compound are considered, as in the case of the MgO series. We have already noted that the Madelung potential shifts the surface oxygen levels towards higher and higher energies and the surface cation levels towards lower and lower energies, in this series. In addition, it also shifts the adsorbate levels with an increasing strength, because of the reduced atomic density in the outer plane (while intra-plane interactions decrease, inter-plane interactions increase). It raises the proton level and lowers the hydroxyl group levels in a more and more efficient way in the series. The energy difference, $\varepsilon_1 - \varepsilon_2$, happens to be roughly constant, both for the proton and the hydroxyl group adsorption. This explains why n_{H+} remains constant on the three surfaces and why the electron transfer *per bond*, $\Delta n_{OH}/Z_a$, is roughly constant for the adsorption of hydroxyl groups.
- the adsorbates also exert an electrostatic potential on the substrate atoms and on each other. The effect is especially noticeable when the adsorbate density is large. By carefully analyzing the changes in the level positions due to this effect,[11] one can rationalize the modifications of charge transfers, between the limit of zero coverage and full saturation.

To summarize, we have stressed in this section that the Lewis acidity depends upon three parameters which are the adsorbate coordination number, Z_a—*i.e.* the number of interfacial bonds per adsorbed molecule—the resonance integrals, β, and the acceptor-donor energy difference, $\varepsilon_1 - \varepsilon_2$, calculated with the intra-atomic and Madelung corrections. These quantities are related to the cation electronegativity, the surface oxygen charge, the oxide structure, the surface orientation and the surface coverage, but the relationship is generally intricate due to the self-consistent link between charges

and potentials, and due to the mutual interaction between the adsorbates and the substrate.

4.3 Adsorption Energies

The adsorption energies involve several contributions, among which the electrostatic (Madelung) energy and the covalent one are the most important.[42-46]

At variance with the electrostatic models, the covalent contribution generally prevails in the strong adsorption processes discussed here, which means that they are driven by the formation of covalent interfacial bonds. A generalization of equation (7.13) in the appendix allows one to write the covalent energy in the following way:

$$E_{cov} = -4n_0 \frac{Z_a\beta^2}{\sqrt{(\varepsilon_1 - \varepsilon_2)^2 + 4Z_a\beta^2}}. \tag{4.4}$$

It is an increasing function of the ratio $Z_a\beta^2/(\varepsilon_1 - \varepsilon_2)$ (note that, at variance with the charge transfer expression, the energy difference in the denominator is not squared). In the limiting case where β is much smaller than $\varepsilon_1 - \varepsilon_2$, this gives back the expressions found in Mulliken's and Hudson's and Klopman's works.[42-46] The parameters on which the ratio $Z_a\beta^2/(\varepsilon_1 - \varepsilon_2)$ relies have already been discussed above. As far as the surface-OH^- bond is concerned, the covalent energy is weak on basic oxides and strongly increases on acidic oxides. This behaviour is consistent with the values of the charge transfers which have been discussed above and can be explained with the same arguments—increasing electronegativity, decreasing ionic radius, increasing Madelung potentials. Similarly, on the three MgO surfaces, despite the fact that the charge transfer on each Mg-OH bond is roughly constant, the formation of 1, 2 and 3 bonds in the series induces an increase of the *total* charge transfer and of the covalent energy. A simple model of chemisorption, in the limit of weak coupling, displays the same trends for metallic surfaces.[47,48]

The electrostatic energy, on the other hand, is not simply equal to the direct charge-charge interaction between the adsorbate and the surface atom on which it adsorbs, as assumed in Parks' or MUSIC models, because of the long-range nature of the Coulomb interactions and because of the presence of the adsorbate-substrate charge transfers. Several points have to be noticed:

- The adsorbate-substrate interaction is the result of attractive and repulsive forces exerted by all the substrate ions: it is much smaller than the interaction with a single ion; for example, on MgO(100), assuming integer charge values, the proton-oxygen interaction energy is of the order of 30 eV, *i.e.* about fifteen times larger than the interaction between the proton and the whole substrate. In addition, it has to be estimated, not with the ionic formal charges, but with the effective charges resulting from the oxygen-cation electron sharing in the substrate.
- The adsorbate-substrate charge transfer is responsible for a reduction of the charges of both species: the hydroxyl groups and surface oxygens lose electrons while protons and surface cations capture electrons. This reduces the direct adsorbate-substrate interaction, and the effect is stronger and stronger as the covalency of the interfacial bond gets larger.

- The charge decrease on the substrate adsorption site also modifies the electrostatic interactions *inside* the substrate. The cohesion of this latter decreases: for a given charge transfer, the effect is larger on surfaces with lower Miller indexes. We have found that the increase of $E_{H^+}^{ads}$ in the series of the three MgO surfaces may be explained in that way. This is an example in which one would conclude that the oxygen basicity does not depend upon the surface orientation, on the basis of charge transfer considerations, while adsorption energy considerations lead to an increasing basicity in the series.

This discussion also shows that neither the covalent nor the electrostatic energies can be written as simple products of parameters characterizing the acid A and the base B, as postulated in the Drago and Wayland[49] $E\&C$ equation:

$$-\Delta H = E_A E_B + C_A C_B. \tag{4.5}$$

The properties of the coupled system—for example the number of formed bonds between the adsorbate and the substrate or the substrate decohesion which results from the charge transfer—are also important. The same remarks apply to the model of adhesion proposed by Bolger which expresses the adhesion energy as the difference between two energies characteristic of the reactants in the absence of each other.[14]

The trends found for adsorption energies in the various series do not systematically coincide with those found on charge transfers, thus revealing a sensitivity of the acidity scales to the parameter on which they are based: this is true, for example, for the proton adsorption on MgO in the limit of zero coverage. It comes from the fact that the contributions to the adsorption energy vary with the charge transfers neither in a proportional nor in a monotonic way; the oxide acidity scale thus depends upon whether one uses a charge transfer criterion (Lewis' acidity) or an adsorption energy criterion (*IEPS*, adsorption of test molecules, etc.). The systematic study of the adsorption of more complex molecules on model surfaces should allow one to refine this analysis in the future.

4.4 Structural Characteristics of Surface OH Groups

We now discuss the relationship between the surface acidity and the structural characteristics of surface OH groups, the O—H inter-atomic distance and the stretching frequency, ν_{OH}.

As a general statement, it is recognized that, when a chemical bond forms, the dependence of the bond energy as a function of the bond length presents systematic features: for example, the deeper the well in the energy curve, the larger the curvature. A universal model, accounting for these features, was proposed for metallic cohesion, adsorption and adhesion processes[50] and specified in the particular case of transition metals.[51] It relies upon the assumption that the adsorption energy results from a competition between an attractive interaction and a short range repulsion term, the latter varying with the bond length more rapidly than the former ($n > m$).

In the context of acid-base interactions, systematic relationships between the bond lengths, the charge transfers and the coordination numbers have also been noted and qualitative rules have been established.[52, 53]

It is possible to develop a theoretical model for the O—H bond which includes these characteristics. It relies upon the assumption that, as a first approximation, the covalent term is the attractive term whose distance dependence is the strongest. To derive its dependence upon n_H, we consider the simple model of an O—H bond, in which only the hydrogen 1*s* orbital $|H\rangle$ and the oxygen p_z orbital $|O\rangle$ are hybridized; the resonance integral is denoted β. The wave function, ψ_B, of the OH bonding state is expanded on these two orbitals:

$$\psi_B = x|O\rangle + y|H\rangle \tag{4.6}$$

with $x^2 + y^2 = 1$. The covalent energy, E_{cov}, equal to twice the expectation value of the non-diagonal part of the Hamiltonian, H_{ND}: $E_{cov} = 2\langle\psi_B|H_{ND}|\psi_B\rangle$, is equal to $E_{cov} = 4xy\beta$ and the hydrogen electron number reads $n_H = 2y^2$. The covalent energy is, thus, expressed as a function of n_H in the following way:

$$E_{cov} = -2|\beta|\sqrt{n_H(2-n_H)} \tag{4.7}$$

Assuming that the resonance integral varies as an inverse power law with the O—H distance, *d*, the *d*-dependent part of the O—H bond energy thus reads:

$$E = -\frac{B\sqrt{n_H(2-n_H)}}{d^m} + \frac{A}{d^n} \tag{4.8}$$

The O—H bond energy, bond length and stretching frequency are, thus, respectively proportional to:

$$E_{OH} \propto [n_H(2-n_H)]^{\frac{n}{2(n-m)}} \tag{4.9}$$

$$d_{OH} \propto \left[\frac{1}{n_H(2-n_H)}\right]^{\frac{1}{2(n-m)}} \tag{4.10}$$

$$\nu_{OH} \propto [n_H(2-n_H)]^{\frac{n+2}{4(n-m)}}. \tag{4.11}$$

Their variations as a function of n_H are represented on Figure 1, after normalization to the free hydroxyl group characteristics (for which $n_H = 0.97$ in this approach). Short bond lengths and high stretching frequencies are, thus, associated with strong bonds, for which the charge transfers, n_H, are large. In the specific case of OH species, this model thus provides an analytical basis to the qualitative rules established in the acid-base literature.[52, 53]

Equations (4.9)–(4.11) make the link between the oxygen Lewis basicity–*i.e.* the ability of the oxygen to give electrons to the hydrogen atom, measured by n_H– and the O—H bond length or stretching frequency. High stretching frequencies are, thus, expected for protons adsorbed on basic surface oxygens or for OH groups weakly interacting with surface cations: this happens because the stronger the substrate-OH bond, the weaker the O—H bond; on surfaces with strongly acidic cations, hydroxyl groups with high stretching frequencies are found. According to the calculations performed on MgO(100), the OH group adsorbed on surface magnesiums should have the highest stretching frequency, because, although strong, the proton-surface is still weaker than that in the free OH^- molecule. This result is in agreement with experimen-

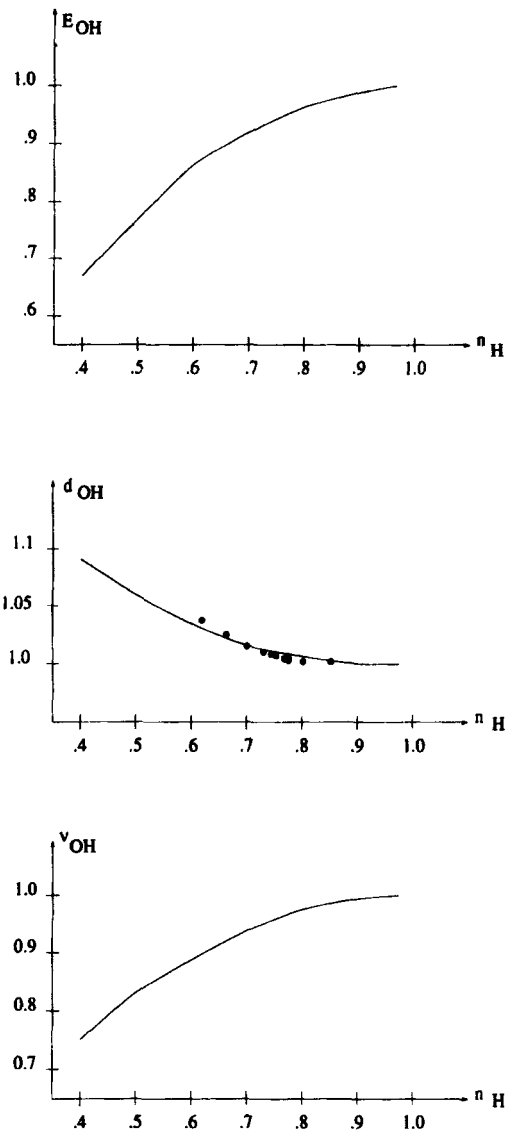

FIGURE 1 Binding energy, E_{OH}, equilibrium inter-atomic distance, d_{OH}, and stretching frequency, ν_{OH}, of the OH bond as a function of the electron number, n_H, borne by the hydrogen atom, according to Equations (4.9)–(4.11). Each quantity is normalized to that characteristic of the free hydroxyl group ($n_H = 0.97$): the exponents of the covalent and repulsion term are taken equal to $m = 2$ and $n = 4.5$. The dots on the second curve correspond to the numerical results given in Table VIII.

tal results.[28, 54] The relationship between the bond length and the charge transfer is similar in spirit to that between the interatomic distances and the bond valences[55] noted in inorganic crystals.

The structural characteristics of OH groups depend upon the density of adsorbates. In particular, on the fully-hydroxylated MgO(100) surface, the interaction between

adsorbates induces a decrease of the oxygen-proton charge transfer, and an expansion of the bond length. According to Equations (4.9)–(4.11), a shift of the stretching frequency towards lower values should result. The dependence of the structural properties of OH groups as a function of the adsorbate density is generally not well apprehended in the literature.

5 CONCLUSION

Relying on the results of model calculations of proton and hydroxyl group adsorption, we have discussed the acid-base strength of various planar oxide surfaces, on the basis of three criteria: the adsorbate-substrate charge transfers, the adsorption energies and the structural properties of adsorbed OH groups. The planar surfaces, considered here, represent simple prototypes of solid acids or bases. They exemplify how the understanding of acidity becomes complicated by solid state effects: the variety of adsorption sites on a given surface, the variety of surface sites as a function of the surface orientation, the long range electrostatic fields, etc. The numerical results show that the trends found for adsorption energies do not coincide systematically with those found on charge transfers, thus revealing a sensitivity of the acidity scales to the parameter on which they are based.

We have discussed the relevance of various microscopic parameters, which determine the Lewis and Brønsted acid-base strength of the surface sites. We have stressed that the surface acidity depends upon quantities which are related, in an intricate way, to the cation electronegativity, the surface oxygen charge, the oxide structure, the surface orientation and the surface coverage. We have shown that it is necessary to consider the oxygen and cation electronegativities, not only in their proper charge states in the oxide, but also modified by the Madelung potential exerted by all the neighboring charges. This introduces a concept of electronegativity *in the solid*. We have also shown that an analytical quantum formulation of the ionicity of the oxygen-cation bond in oxides and of the adsorbate charge transfer is available, which extends earlier approaches based on empirical arguments or perturbative approaches. As far as adsorption energies are concerned, we have pointed out the inadequacy of pure electrostatic models and we have stressed some limitations of simple acid-base models. We have proposed a simple analytical model which assesses the link between the surface acidity and the structural characteristics of the surface OH groups.

The analysis performed in this paper shows that the answer to the first question: "which are the specific properties of the reactants that determine the strength of an acid-base reaction" is not easy. On the one hand, obviously the substrate and adsorbate acceptor and donor level positions are relevant for the interfacial bond formation, their effective charges govern the electrostatic interactions and the cation electronegativity is a key parameter in determining the covalency of the substrate cation-oxygen bond and of the interfacial bond, as recognized in the acid- base literature. On the other hand, we have found a number of examples which prove that the adsorption characteristics cannot be solely predicted on the basis of the isolated adsorbate and substrate properties. The mutual influence of the adsorbates and substrate is an important factor, which may drive the trends for some series. It shifts the frontier orbital energies—*e.g.* the case of proton adsorption on MgO(100), (110) and (211)—it determines the

multiplicity of the bond ($Z_a = 1, 2, 3$) as a function of the reactant geometry and chemical type. It may yield structural distortions in the surface and in the adsorbate. It is especially important when the density of adsorbates is large.

This study represents a first step in the quantum analysis of acid-base reactivity of oxide surfaces, which have been much less studied than the metallic surfaces. It is restricted to ideal surfaces and very small adsorbates, due to the computation times involved. To go closer to experimental conditions met in catalysis or adhesion, obviously less perfect surfaces and more complicated adsorbates should be considered in the future. Quantum approaches, such as the one which is presented here, will not be able soon to compete with empirical acid-base approaches in the prediction of adhesion for the applications. Nevertheless, because they allow a detailed understanding of model situations, they can give hints on how to monitor the acid strength of surfaces, for example by favoring specific surface orientations, or by introducing selected and controlled densities of structural or chemical defects.

6 REFERENCES

1. F. M. Fowkes, *J. Adhesion Sci. Tech.* **1,** 7 (1987).
2. K. L. Mittal and H. R. Anderson, Jr., Eds., *Acid-Base Interactions: Relevance to Adhesion Science and Technology* (VSP BV, Utrecht, The Netherlands, 1991), and references therein.
3. K. Tanabe, *Solid Acids and Bases* (Academic Press, New York, London, 1970).
4. K. Tanabe, in *Catalysis, Science and Technology*, M. Boudert and J. R. Anderson, Eds. (Springer Verlag, Berlin, Heidelberg, New York, 1981), Chap. 5.
5. J. N. Israelachvili, *Intermolecular and surface forces, with applications to colloidal and biological systems* (Academic Press, New York, London, 1985).
6. L. H. Lee in Ref. (2), (1991) p. 25, and references therein.
7. S. R. Cain in Ref. (2), (1991) p. 47, and references therein.
8. V. E. Henrich and P. A. Cox, *The surface science of metal oxides* (Cambridge University Press, 1994).
9. J. Goniakowski, S. Russo and C. Noguera, *Surf. Sci.* **284,** 315 (1993).
10. J. Goniakowski and C. Noguera, *Le Vide, les Couches Minces* Suppl. **272,** 74 (1994).
11. J. Goniakowski and C. Noguera, *Surf. Sci.*, accepted (1995).
12. G. A. Parks, *Chem. Rev.* **65,** 177 (1965).
13. A. Auroux and A. Gervasini, *J. Phys. Chem.* **94,** 6371 (1990).
14. J. C. Bolger, in *Adhesion aspects of polymeric coating*, K. L. Mittal, Ed. (Plenum Press, New York, 1983), p. 3.
15. M. Nabavi, O. Spalla and B. Cabanne, *J. Colloid Interf. Sci.* **160,** 459 (1993).
16. T. Hiemstra, W. H. Van Riemsdijk and G. H. Bolt, *J. Colloid and Interf. Sci.* **133,** 91 (1989).
17. T. Hiemstra, J. C. M. De Wit and W. H. Van Riemsdijk, *J. Colloid and Interf. Sci.* **133,** 105 (1989).
18. L. Pauling, *J. Am. Chem. Soc.* **51,** 1010 (1929).
19. L. Pauling, *The Nature of the Chemical Bond*, 3rd edition (Cornell Univ. Press, Ithaca, New York, 1960), Chap. 13.
20. R. P. Iczkowski and J. L. Margrave, *J. Am. Chem. Soc.* **83,** 3547 (1961).
21. K. Tanaka and A. Ozaki, *J. Catal.* **8,** 1 (1967).
22. G. Connell and J. A. Dumesic, *J. Catal.* **101,** 103 (1986).
23. G. Connell and J. A. Dumesic, *J. Catal.* **102,** 216 (1986).
24. R. T. Sanderson, *Inorg. Chem.* **3,** 925 (1964).
25. K. Tanabe and Y. Fukuda, *React. Kinet. Catal. Lett.* **1,** 21 (1974).
26. R. T. Sanderson, in *Chemical Periodicity* (Rheinhold, New York 1960).
27. H. P. Boehm, *Discuss. Faraday Soc.* **52,** 264 (1971).
28. T. Shido, K. Asakura and Y. Iwasawa, *J. Chem. Soc. Faraday Trans. I* **85,** 441 (1989).
29. B. A. Morrow, *Stud. Surf. Sci. Catal.* **A57,** 161 (1990).
30. H. Vinek, H. Noller, M. Ebel and K. Schwarz, *J. Chem. Soc. Faraday Trans. I* **73,** 734 (1977).
31. W. M. Mullins and B. L. Averbach, *Surf. Sci.* **206,** 41 (1988).
32. M. Delamar, *J. Elec. Spect. Rel. Phen.* **53,** c11 (1990).

33. M. Casamassima, E. Darque-Ceretti, A. Etcheberry and M. Aucouturier, *Appl. Surf. Sci.* **52,** 205 (1991).
34. J. Goniakowski and C. Noguera, *Surf. Sci.* **319,** 81 (1994).
35. C. Noguera, *Physique et Chimie des Surfaces d'oxydes* (Eyrolles, Paris; collection Alea Saclay) (1995); the English version of this book is in press (Cambridge University Press) (1995).
36. M. Bensoussan and M. Lannoo, *J. Physique (France)* **40,** 749 (1979).
37. J. P. Julien, D. Mayouand F. Cyrot-Lackmann, *J. Physique (France)* **50,** 2683 (1989).
38. J. Goniakowski and C. Noguera, *Surf. Sci.* **319,** 68 (1994).
39. J. Goniakowski and C. Noguera, submitted to *Surf. Sci.* (1995).
40. J. D. Levine and P. Mark, *Phys. Rev.* **144,** 751 (1966).
41. D. E. Parry, *Surf. Sci.* **49,** 433 (1975).
42. R. S. Mulliken, *J. Chem. Phys.* **19,** 514 (1951).
43. R. S. Mulliken, *J. Chem. Phys.* **56,** 801 (1952).
44. R. S. Mulliken, *J. Am. Chem. Soc.* **74,** 811 (1952).
45. R. F. Hudson and G. Klopman, *Tetrahedron Lett.* **12,** 1103 (1967).
46. G. Klopman and R. F. Hudson, *Theor. Chim. Acta* **8,** 165 (1967).
47. M. C. Desjonquères and D. Spanjaard, *J. Phys. C: Solid State Phys.* **15,** 4007 (1982).
48. M. C. Desjonquères and D. Spanjaard, *J. Phys. C: Solid State Phys.* **16,** 3389 (1983).
49. R. S. Drago and B. B. Wayland, *J. Am. Chem. Soc.* **87,** 3571 (1965).
50. H. Rose, J. R. Smithand J. Ferrante, *Phys. Rev. B* **28,** 1835 (1983).
51. D. Spanjaard and M. C. Desjonquères, *Phys. Rev. B* **30,** 4822 (1984).
52. I. Lindqvist, *Inorganic adduct molecules of oxo-compounds* (Springer-Verlag, Berlin, Göttingen, Heidelberg, 1963).
53. V. Gutmann, *The donor-acceptor approach to molecular interactions* (Plenum Press, New York, London, 1978).
54. V. Coustet and J. Jupille, *Surf. Interf. Anal.* to be published.
55. I. D. Brown, *Acta Cryst. B* **33,** 1305 (1977).

7 APPENDIX

We give in this Appendix the main steps of an analytical model which accounts for the mixed iono-covalent character of the oxygen-cation bond in insulating oxides and yields Equation (4.3) for the partial charges and Equation (4.4) for the covalent energy.

It is a tight-binding approach, suited to binary oxides of stoichiometry M_nO_m, in which the atoms occupy the sites of an alternating lattice. The eigenfunctions of the Hamiltonian are expressed as a linear combination of atomic orbitals; the basis set is assumed to be othonormal. Two basic assumptions underlie the model:

- all the cation (oxygen) outer levels have the same energy, ε_M (respectively, ε_O for the oxygens); their degeneracy is noted $d_M(d_O)$. The crystal field splitting is thus neglected, and so is the energy difference between the various atomic orbitals which are involved in the chemical bond (*e.g.* 3*d* and 4*s* for titanium in TiO_2).
- orbital hybridization takes place only between first neighbor atoms of opposite type. Resonance integrals, thus, connect one sub-lattice to the other as a result of the alternating character of the lattice.

The Hamiltonian, H, can be split into two parts: a diagonal part, H_D, which involves the site energies ε_O and ε_M, and a non-diagonal part, H_{ND}, associated with the resonance integrals. The eigenfunctions, $|\psi_k\rangle$:

$$H|\psi_k\rangle = E_k|\psi_k\rangle \tag{7.1}$$

are equal to the sum of two components, $|\psi_{kO}\rangle$ and $|\psi_{kM}\rangle$, which represent the projection of $|\psi_k\rangle$ on the oxygen and cation sub-lattices. When projected on $|\psi_{kO}\rangle$ and

$|\psi_{kM}\rangle$, Equation (7.1) yields two coupled equations:

$$H_{ND}|\psi_{kO}\rangle = (E_k - \varepsilon_M)|\psi_{kM}\rangle \tag{7.2}$$

$$H_{ND}|\psi_{kM}\rangle = (E_k - \varepsilon_O)|\psi_{kO}\rangle \tag{7.3}$$

which, after a second application of H_{ND}, lead to the effective Schrödinger equations:

$$H_{ND}^2|\psi_{kO}\rangle = (E_k - \varepsilon_O)(E_k - \varepsilon_M)|\psi_{kO}\rangle \tag{7.4}$$

$$H_{ND}^2|\psi_{kM}\rangle = (E_k - \varepsilon_O)(E_k - \varepsilon_M)|\psi_{kM}\rangle \tag{7.5}$$

The eigenstate problem is, thus, equivalent to finding the eigenfunctions, $|\psi_{kO}\rangle$ and $|\psi_{kM}\rangle$, and eigenvalues, $F_k = (E_k - \varepsilon_O)(E_k - \varepsilon_M)$, of H_{ND}^2 on one sub-lattice. Due to the positive definite character of the operator H_{ND}^2, all the F_k values are larger than or equal to zero.

Once the solutions of H_{ND}^2 are obtained, *i.e.* after the determination of the band dispersion, F_k, of the range of existence of F_k: $[F_{min}, F_{max}]$ and of the density of states, $M(F)$, it is possible to deduce the total $N(E)$ and local densities of states, $N_O(E)$ and $N_M(E)$, on the oxygen and cation sub-lattices, thanks to the following relationships:

$$N(E) = 2\left|E - \frac{(\varepsilon_M + \varepsilon_O)}{2}\right| M(E) + n_1\delta(E - \varepsilon_M) \tag{7.6}$$

and:

$$N_O(E) = |E - \varepsilon_M| M(E) \tag{7.7}$$

$$N_M(E) = |E - \varepsilon_O| M(E) + n_1\delta(E - \varepsilon_M) \tag{7.8}$$

In the expression for $N(E)$, one has used the equality, $F = (E - \varepsilon_O)(E - \varepsilon_M)$, and $M(E)$ is the transcription of $M(F)$ by the change of variable F into E. For definiteness, we have assumed that $md_O < nd_C$, and we have denoted $n_0 = \min(nd_C, md_O)$ and $n_1 = \max(nd_C, md_O) - n_0$. With each eigenvalue, F_k, are associated two energies, $E_k^{\pm}$, equal to:

$$E_k^{\pm} = \frac{(\varepsilon_M + \varepsilon_O)}{2} \pm \frac{1}{2}\sqrt{(\varepsilon_O - \varepsilon_M)^2 + 4F_k} \tag{7.9}$$

The $-$ sign refers to the valence band and the $+$ sign to the conduction band.

To obtain information on the oxygen-cation charge transfer and on the band energy, one has to assume an approximate expression of $M(F)$. The simplest form is a delta function peaked at the energy, F, of its first moment. Due to the quadratic relationship between F_k and E_k, the first moment of $M(F)$ on the oxygen sub-lattice is equal to the covalent contribution to the second moment of $N_O(E)$, *i.e.* $Z\beta^2$, with Z the oxygen coordination number:

$$M(F) = n_0\delta(F - Z\beta^2) \tag{7.10}$$

The assumption made for $M(F)$ amounts to considering only local hybridization and neglecting long-range band effects. One may then write the total and local densities of

states using Equations (7.6)–(7.8). For example:

$$N_O(E) = n_0 \frac{(x + \sqrt{4Z\beta^2 + x^2})}{2\sqrt{4Z\beta^2 + x^2}} \delta\left(E - \frac{\varepsilon_M + \varepsilon_O}{2} + \sqrt{Z\beta^2 + x^2/4}\right)$$
$$+ n_0 \frac{(\sqrt{4Z\beta^2 + x^2} - x)}{2\sqrt{4Z\beta^2 + x^2}} \delta\left(E - \frac{\varepsilon_M + \varepsilon_O}{2} - \sqrt{Z\beta^2 + x^2/4}\right) \quad (7.11)$$

with $x = \varepsilon_M - \varepsilon_O$. The total and local densities of states display two peaks located at symmetric positions with respect to $(\varepsilon_O + \varepsilon_M)/2$.

The integration of $N_O(E)$ over the valence band yields the oxygen electron number; the absolute value, $|Q_O|$, of the oxygen charge is equal to:

$$|Q_O| = 2 - \frac{n_0}{m}\left(1 - \frac{\varepsilon_M - \varepsilon_O}{\sqrt{(\varepsilon_M - \varepsilon_O)^2 + 4Z\beta^2}}\right) \quad (7.12)$$

The covalent energy is obtained by integration of $EN(E)$ over the valence band, and subsequent subtraction of the atomic energy, $N_O\varepsilon_O + N_M\varepsilon_M$:

$$E_{cov} = -4n_0 \frac{Z\beta^2}{\sqrt{(\varepsilon_M - \varepsilon_O)^2 + 4Z\beta^2}} \quad (7.13)$$

which may also be written:

$$E_{cov} = -2m|\beta|\sqrt{Z}\sqrt{\delta Q\left(2\frac{n_0}{m} - \delta Q\right)} \quad (7.14)$$

as a function of the oxygen-cation electron transfer, $\delta Q = 2 - |Q_O|$